Simultaneous Differential Diffusion under Weak Turbulence

A. RUIZ-ANGULO[1]

[1]Department of Mechanical Engineering, California Institute of Technology, Pasadena, CA 91106, USA

(Received 14 December 2007)

We present the results from experimental measurements of simultaneous fluxes of heat and salt across an interface of a diffusively stable bi-layer system. Turbulence was generated inside each of the layers by oscillating grids. Time series of temperature and salinity were taken until both properties came to equilibrium.

1. Introduction

The density of sea-water, ρ_{sw}, is a function of temperature, T, and salinity, S. In the ocean, when mixing of density surfaces occur (diapycnal), temperature and salinity mix as well. The two properties could either mix at the same rate or at a different rates. In the presence of turbulence, the larger molecular diffusivity of T might create a preferential turbulent transfer relative to S. However, the usual formulas used in numerical models of the ocean specify a transfer independent of diffusivity. If diffusion is incorporated, this process is often called *differential diffusion*.

The more familiar *double diffusion* convection has two important regimes based on the density ratio (R_ρ): $R_\rho = \alpha\partial T\partial z/\beta\partial Sz > 1$ corresponding to the *finger regime* and $R_\rho = \beta\frac{\partial S}{\partial z}/\alpha\frac{\partial T}{\partial z} > 1$ for the *diffusive regime* (Turner (1979)). The *diffusive* and *finger* regimes lead to differential diffusion by imposing 'ordinary' turbulence, i.e., the kinetic energy driving the the double diffusion is supplied. Turner (1968) and Linden (1971) found that the convective finger regime could be accelerated and both properties, temperature and salinity mixed at the same rate for small Ri. The experiments showed that the action of the turbulence could overcome the heat flux due to the fingers.

Numerical simulations of turbulent mixing models ignore the fact that temperature and salinity might transport differentially, arguing that for low Richardson number, Ri, heat and salt fluxes produce an effective coefficient of eddy diffusivity $\kappa \sim 1$. On the other hand, for weakly turbulent flows –low to moderate Ri– the diffusivity ratio, κ_T/κ_S (where κ_T and κ_S are the eddy diffusivities for salt and heat) is less than 1 (Jackson & Rehmann (2003*b*), Gargett *et al.* (2003)). It has been show as well (Jackson & Rehmann (2003*a*)) that the mixing efficiency is sensitive to the eddy diffusivity; therefore, considering $\kappa = 1$ would represent an error on calculations were the mixing regime is not strenuously turbulent, i.e., $Ri > 1$.

Recent work has led to a greatly improved understanding of this phenomenon. Zellouf *et al.* (2005) presented experiments on single density stratified interface configurations, where salt and heat fluxes are calculated separately. By finding an effective Richardson number, Ri, based on the turbulence generated by two grids oscillating on each of the stable layers they showed that the heat and salt buoyancy fluxes in stratified fluid grid

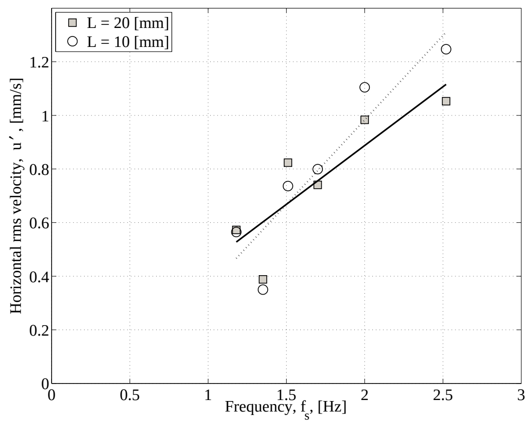

FIGURE 1. Horizontal rms velocity as a function of the grids frequency. The zero reference corresponds to the initial location of the stratified interface. The length L is measured symmetrically from the zero reference

turbulence possessed two different responses to the mixing. This is similar to that in a double-diffusive convection system.

Even for configurations where T and S are stable, there is potential for differential transport of T and S (Merryfield *et al.* (1998)). The objective of the present work is to document wether the buoyancy fluxes of heat and salt under mild turbulence are the same or are different.

2. Experimental setup and technique

Induced mixing experiments were carried out for a diffusively stable bi-layer system. Before each experiment, half of an insulated tank was filled up with *cold* and *salty* water. On top of that layer, *fresh* and relatively *warm* water was slowly poured over a floating sponge, producing a sharp interface between the two layers. Two grids previously located in the middle of each layer were oscillated to produce turbulence. The turbulence intensity is a linear function of the oscillating frequency (see Figure 1).

2.1. *Experimental apparatus*

All the experiments were conducted in an insulated container made out of styrofoam, the inner dimensions of the tank were $300 \times 300 \times 300$ [mm], the thickness of the walls were 25.7 [mm].

For this experiment, the heavier *cold and salty* fluid was poured into the tank first and then the lighter *warm and fresh* fluid was carefully poured on top of the first layer. The lighter fluid was slowly pumped onto a floating sponge in order to minimize the mixing at the interface. Figure 3 sketches a typical interface between the two layers. In every case both layers were of equal depth, 150 [mm]. In these experiments the interface between the two fluids remained sharp and stable before any oscillations commenced. For all the analysis the molecular diffusion was neglected. The main goal of this work was to look at the mixing driven by weak turbulence. Although in the absence of turbulence the mixing thickness for such a stable configuration grows as $O(1/\sqrt{t})$, all the experiments started soon after the top layer was completed.

The two grids that generated the turbulence were machined out of a Plexiglas plate,

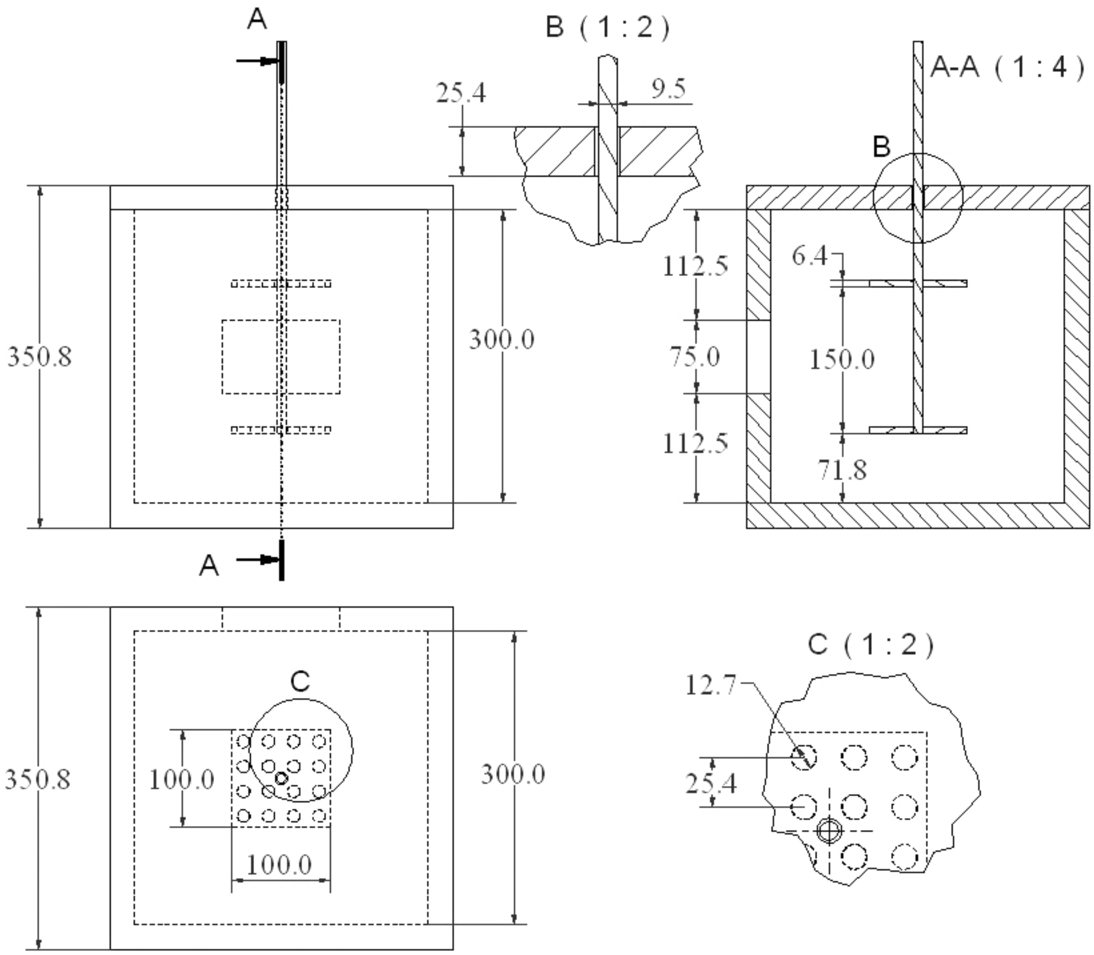

FIGURE 2. Experimental apparatus. The upper left panel corresponds to one side view of the experiment, the section $AA\prime$ represents a cut right in the centre of the apparatus. The thickness of the walls is uniform, 25.4 [mm]. The location of the grids correspond to the centre of each layer. The two grids are identical and a detailed picture with the distribution of the holes is shown. The detail B shows the top cover of tank and the rod which was coupled to an electric motor. The lower left panel is the top view of the apparatus.

of thickness 6.43 [mm] and dimensions 100 × 100 [mm]. Figure 2 shows a sketch of the grid geometry, 16 holes of 12.7 [mm] in diameter were equally distributed on the plate, the separation between centers was 25.7 [mm]. The two grids were connected from the center by a long rod with 9.52 [mm] in diameter. The location of the grids was at the centre of each stratified layer where they simultaneously oscillated. Note that both grids were 75 [mm] away from the interface.

The rod was coupled to a mechanism which converted the rotational motion from an electric motor into a periodic linear vertical displacement. The displacement length, the stroke, was set to 10 [mm] for all the experiments. The motor was connected to a variable speed device which allowed us to adjust the grid oscillating frequency. For all the experiments the oscillating frequency ranged from $1-3$ [Hz]. The precision of this controlling device combined with the friction of the mechanism produced errors in the frequency around 10%. For each experiment, the oscillating frequency was measured

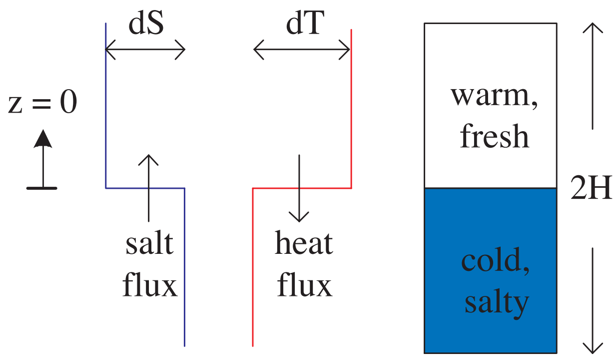

FIGURE 3. Initial temperature and salinity profiles. The configuration presented is diffusively stable. The interface is set to be the zero reference, the total depth of the tank is 2H.

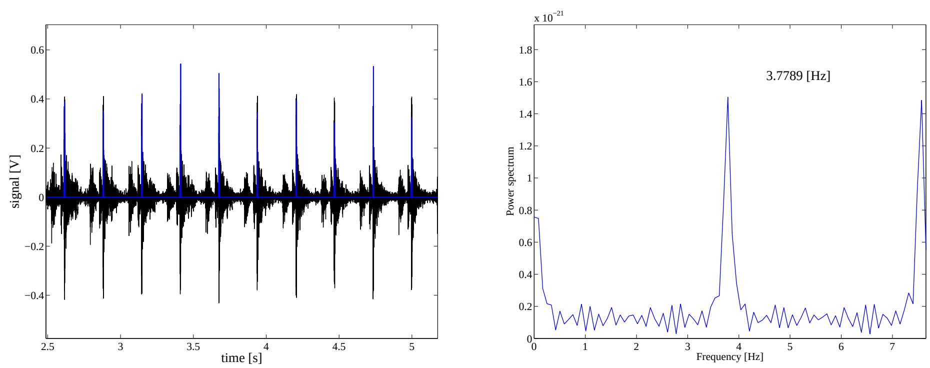

FIGURE 4. Recorded sound signal and the resulting filtered one (left panel), the corresponding characteristic frequency obtained by using a typical Fast Fourier Transform (FFT).

by recording the sound produced by the mechanism every cycle. The sound signal was recorded, filtered and a simple spectral analysis was performed resulting on the oscillating frequency. This procedure was repeated several times within every single experiment, the average of those measurements corresponded to the grids frequency.

The fluid properties were measured from two fixed points located symmetrically about the interface. Two syringes were placed at the hypothetical centre of each layer, 150 [mm] apart. Similarly, two thermometers were placed at the same height as the syringes, sharing the same $x - y$ plane.Time series of temperature and density were simultaneously taken at those two fixed locations.

The temperature changes of each layer were tracked by using a HOBO temperature logger accurate up to 0.01 [^{o} C] . For all the experiments, the sampling rate was 2 [samples/s]. Both thermistors were programed to start at the same time, their internal watch corresponded to real time. The evolution of the density with time was tracked by taking samples of water from the two syringes placed at the centre of each layer. In order to compare density and temperature time series, an external watch was synchronized with the internal watch of the thermistors. The sampling rate for the density varied for all the experiments, approximately $1 - 2$ samples every 10 [min]. The sampled fluid was then analyzed separately with the Anton-paar density meter. The experiment was constantly running at the same rate for several hours until the quantities approached equilibrium,

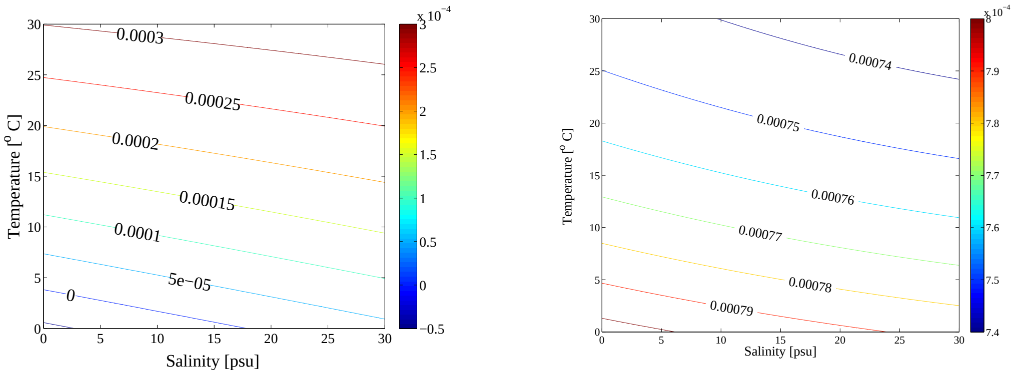

FIGURE 5. Variations of α (left) and β (rigth) with of temperature and salinity at a constant pressure (atmospheric). The range of values for T and S spans the experiments presented in this work
.

those times ranged from $1 - 3.5$ [hrs]. The heat losses through the wall were neglected. The insulation quality of the tank was tested . Therefore, the heat flux with the exterior was ignored within each experiment.

3. Experimental observations

The initially stable layer, represented in Figure 3, gradually changed once the grids started oscillating, small incursions of fluid from the lower and upper layer crossed the interface and transport of heat and salt began. The experiment was designed to be symmetric; therefore, the flux of heat and salt through the interface was assumed to be the same for the upper and lower layer.

In order to compare the contribution of density due to temperature and salinity, the quantities were expressed in buoyancy units. The linear relation for density, ρ, as a function of temperature, T, and salt concentration, S, is given by Equation 3.1

$$\frac{\rho(S,T) - \rho_0}{\rho_0} = -\alpha(T - T_0) + \beta(S - S_0) \tag{3.1}$$

The coefficients α, thermal expansion, and β, saline contraction, are functions of P, T, and S. The coefficient α was pretty sensitive to the changes in T and S, whereas β barley changed within the experimental range. Those variations are shown in figure 5.

The initial conditions for all the experiments are shown in Table 1. The density ratio, R_ρ†, is defined by the ratio of the magnitude of density due to the temperature difference

† In order to obtain positive ratio of densities, a minus sign was added since $\Delta\rho < 0$ and $\Delta T > 0$

Experiment number	R_ρ	N, [1/s]	f_s, [1/s]
DD01	0.67	0.72	1.18
DD02	0.49	0.83	2.28
DD03	0.34	0.87	1.76
DD04	0.29	1.69	1.58
DD05	0.29	1.04	1.85
DD06	0.23	1.01	1.72
DD07	0.16	1.36	1.66

TABLE 1. Initial conditions for different experiments. The experiments are sorted by their density ratio, R_ρ. The initial buoyancy frequency, N, and the average oscillating frequency, f_s, are tabulated as well.

across the interface to the density change due to temperature difference,

$$R_\rho = -\frac{\alpha \Delta T}{\beta \Delta S} \tag{3.2}$$

where ΔT and ΔS are the initial temperature and salinity jumps across the interface.

Since the coefficient of thermal expansion is a function of T and S, the density difference due to temperature is defined by $\alpha \Delta T = (\alpha_w T_w - \alpha_c T_c)$. From figure 5 it is possible to observe that the changes in β within the experimental range of T and S are small.

The buoyancy frequency, N^2, is defined by $-(g\Delta\rho)/(\rho_0 H)$, where H is the distance from the interface to the point where the samples are taken, $\Delta\rho$ is the difference in density between the two layers, ρ_0 is the average density and g is the acceleration due to gravity.

The heat flux, F_T across the interface is defined by

$$A\frac{d}{dt}\int_{H/2}^{0} \rho_c c_p T_c dz = F_T A \;=\; -A\frac{d}{dt}\int_{0}^{H/2} \rho_w c_p T_w dz = F_T A \tag{3.3}$$

where A is the area of the interface, c_p is the specific heat at constant pressure, ρ_c and T_c are the density and temperature of the 'cold' layer. Similarly, ρ_w and T_w are the the density and temperature of the 'warm' layer. Due to the symmetry of the experiment, the heat and salt fluxes across the interface should have the same magnitude.

$$A\frac{d}{dt}\int_{H/2}^{0} \rho_0 S_c dz = F_S A \;=\; -A\frac{d}{dt}\int_{0}^{H/2} \rho_0 S_w dz = F_S A \tag{3.4}$$

where S is the salt concentration and the subindices c and w correspond to the cold and warm layers.

3.1. *Differential equilibrium*

The state of equilibrium is defined as the absence of fluctuations on the buoyancy quantities, which corresponds to a fully mixed state. For the combinations presented in this work the equilibrium is reached differently for temperature and salinity.

For a relatively weak stratification and a relatively strong turbulence, the equilibrium is reached at the same time for temperature and salinity (See Figure 6). On the other hand, for relatively strong stratification and weak turbulence, differential diffusion occurs. In Figure 7 it is possible to observe that the buoyancy temperature has reached equilibrium

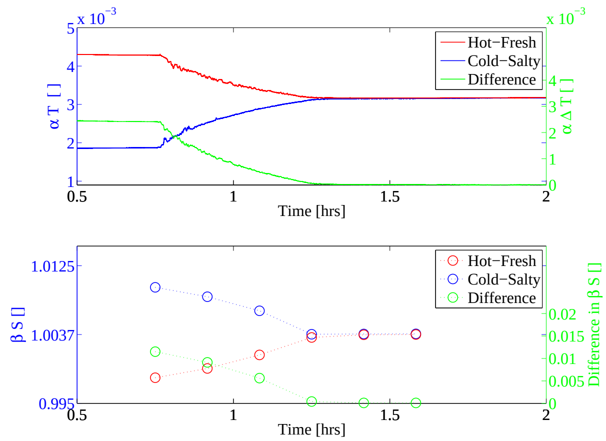

FIGURE 6. Experiment DD03. The upper panel shows the temperature decaying with time and in the lower layer, the corresponding decay of salinity – both in buoyancy units –. The final equilibrium state is about the same for both quantities.

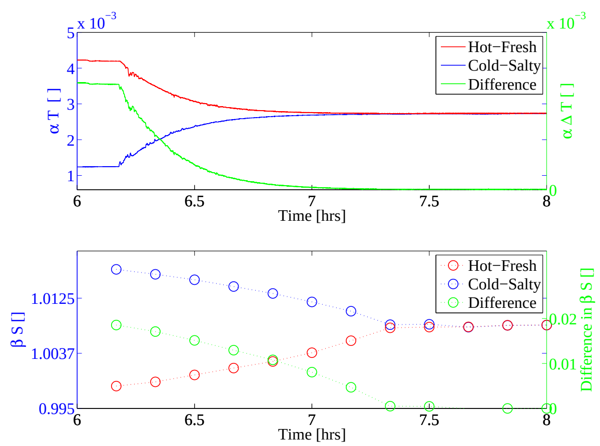

FIGURE 7. Experiment DD06. The upper panel shows the temperature decaying with time and in the lower layer, the corresponding decay of salinity – both in buoyancy units –. The final equilibrium state is different for both quantities.

but the salinity requires more time to become fully mixed. In this case, the differential transport of the properties is clear.

3.1.1. *Constant oscillating frequency*

To isolate the effect of the stratification on the experiments, we carried an experiment where we changed the initial stratification and on average the oscillating frequency remained constant. From Table 1 the experiments taken were: $DD03$, $DD06$ and $DD07$. The $T - S$ evolution is shown in Figure 8 where the blue symbols correspond to the cold and salty layer and the red symbols correspond to the warm and fresh layer. The ordinate corresponds to the temperature in Celsius and the abscissa corresponds to the salinity in *psu* units. The contour lines correspond to iso-density (isopycnals) surfaces.

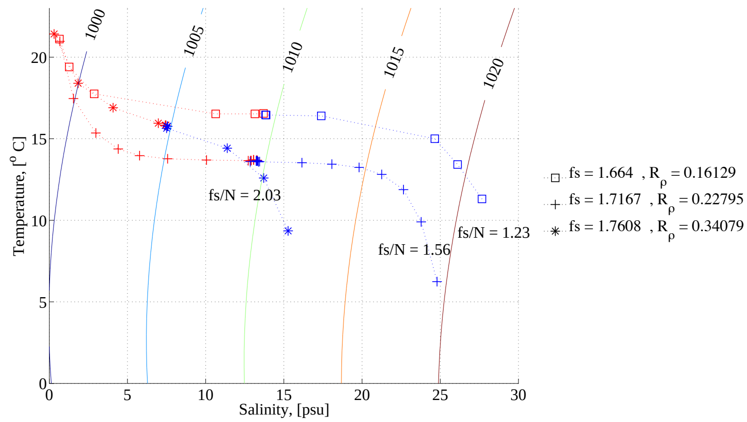

FIGURE 8. $T - S$ diagram for relatively constant oscillating frequencies

.

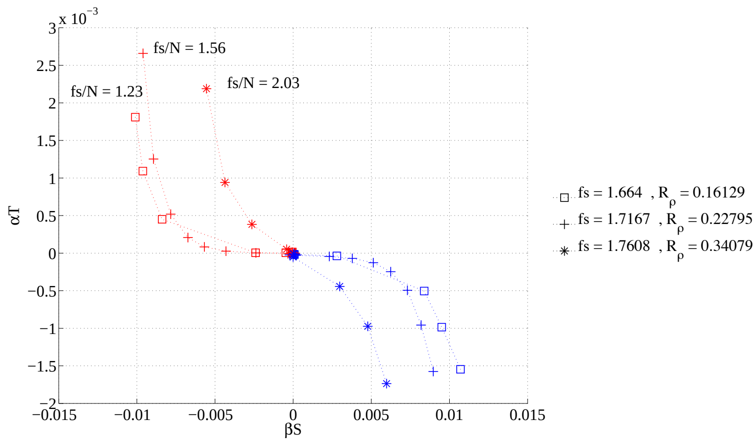

FIGURE 9. $T - S$ diagram in buoyancy units for relatively constant oscillating frequencies

.

Figure 9 shows a similar plot as Figure 8 representing a $T - S$ diagram in buoyancy units. For convenience the origin corresponds to the equilibrium point form both sides, salinity and temperature. The direction of time travels from the extreme on the curves towards the equilibrium point.

For relatively high density ratios (Eq. 3.2) and similar oscillating frequency the temperature and salinity reach equilibrium at similar times. The lower the density ratio, the slower the salinity reaches equilibrium. The ratio of oscillating frequency, f_s, to the initial buoyancy frequency, N, was estimated. The ratio of frequencies is a measurement of the inertia to the stratification strength; therefore, the larger the frequency ratio, the faster the quantities come to equilibrium.

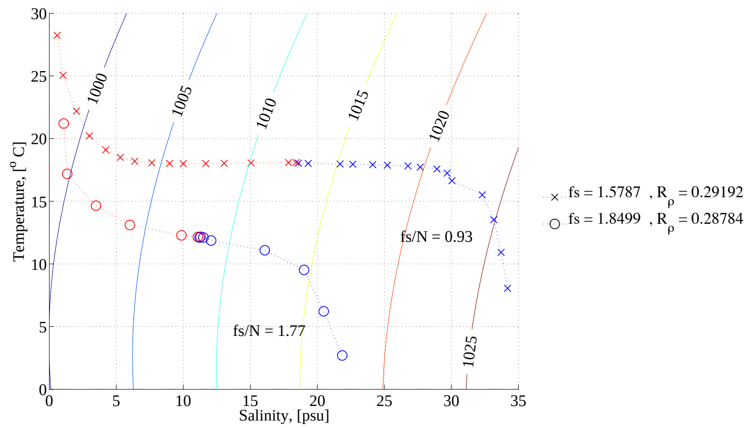

FIGURE 10. $T - S$ diagram for relatively constant density ratios.

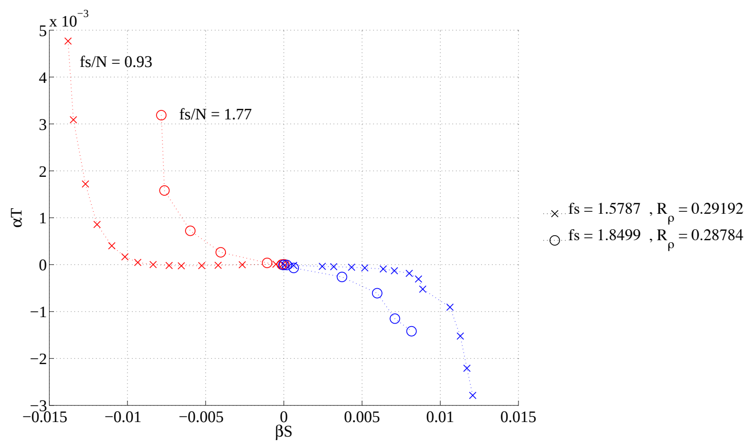

FIGURE 11. $T - S$ diagram in buoyancy units for relatively constant density ratios.

3.1.2. *Constant density ratio*

We now look at the influence of the frequency. Note that for the density ratio to be equal does not mean that the initial conditions are exactly the same. The variations on the oscillating frequency produced the two expected regimes: differential equilibrium and non differential equilibrium. In Figure 11 two different experiments, $DD04$ and $DD05$, are shown. The ratio of densities was constant for the two experiments and the oscillating frequencies were 1.58 and 1.85 Hz. Figure 10 shows the dimensional $T - S$ diagram, $iso - density$ surfaces were superimposed to show that the mixing process crosses those lines until it reaches equilibrium. Similarly to the previous section the larger the ratio of frequencies, the slower the equilibrium is reached.

4. Summary

This study presented controlled laboratory experiments that allowed to observe simultaneously the evolution of the heat and salt fluxes across the interface between two layers. The diffusively stable layers presented for all the experiments were perturbed by symmetrically oscillating two grids in the range of $1.2 < f_s < 2.2$ Hz. The density ratios spanned the range of $0.16 < R_\rho < 0.67$.

We separated the effects in frequency perturbed and density ratio perturbed and we found that for both cases there is a mismatch on reaching the equilibrium for the temperature and for the salinity. We also found that the heat flux decreases monotonically for all the cases, regardless of the value of f_s or R_ρ. On the other hand, the flux of salt tends to be constant for low oscillating frequencies ($DD01$ and $DD04$), for the rest of the experiments the flux of salt increases reaching a maximum approximately at the same time as the heat flux begins to asymptote.

In the absence of a proper Richardson number, the ratio of frequencies seemed to be the right parameter to characterize the differential equilibrium

Combined results from numerical simulations, laboratory experiments and geophysical measurements indicate that, at low (but non-zero) turbulence levels (small Reb), there is a strong tendency for incomplete mixing of salinity when temperature is completely mixed (small d). If this is widespread in the deep ocean, models that mix both constituents at the same rate must be reconsidered.

5. Acknowledgments

Thanks to all the fellows and staff from the GFD program, specially to Jack Whitehead for his guidance and Keith F. Bradley for his help on building and putting together the experiment. Special thanks to George Veronins and Louis Howard for their helpful discussions.

REFERENCES

Gargett, Ann E., Merryfield, William J. & Holloway, Greg 2003 Direct numerical simulation of differential scalar diffusion in three-dimensional stratified flow. *Journal of Physical Oceanography* **33**, 1758–1782.

Jackson, P. Ryan & Rehmann, Chris R. 2003*a* Kinematic effects of differential transport on mixing efficiency in a diffusively stable, turbulent flow. *Journal of Physical Oceanography* **33**, 299–304.

Jackson, P. Ryan & Rehmann, Chris R. 2003*b* Laboratory measurements of differential diffusion in a diffusively stable, turbulent flow. *Journal of Physical Oceanography* **33**, 1592–1603.

Linden, P. F. 1971 Salt fingers in the presence of grid generated turbulence. *Journal of Fluid Mechanics* **49**, 611–624.

Merryfield, W.J., Holloway, Greg & Gargett, Ann E. 1998 Differential vertical transport of heat and salt by weak stratified turbulence. *Geophysical Research Letters* **25** (15), 2773–2776.

Turner, J.S. 1968 The influence of molecular diffusivity on turbulent entrainment across a density interface. *Journal of Fluid Mechanics* **33**, 639–656.

Turner, J. Stewart 1979 *Buoyancy Effects in Fluids*. Cambridge University Press.

Zellouf, Y., Dupont, P. & Peerhossaini, H . 2005 Heat and mass fluxes acress density interfaces in a grid-generated turbulence. *International Journal of Heant and Mass Transfer* **48**, 3722–3735.